

## Research Article

# A Study on a Solar Simulator for Dye Sensitized Solar Cells

**Kyoung-Jun Lee,<sup>1</sup> Jeong-Hoon Kim,<sup>1</sup> Ho-Sung Kim,<sup>1</sup> Dongsul Shin,<sup>1</sup>  
Dong-Wook Yoo,<sup>2</sup> and Hee-Je Kim<sup>1</sup>**

<sup>1</sup> Department of Electrical Engineering, Pusan National University, Jangjeon, Geumjeong, Busan 609-735, Republic of Korea

<sup>2</sup> Power Conversion Center, HVDC Division, KERI, Changwon, Republic of Korea

Correspondence should be addressed to Hee-Je Kim, heeje@pusan.ac.kr

Received 27 October 2011; Accepted 27 December 2011

Academic Editor: Bhushan Sopori

Copyright © 2012 Kyoung-Jun Lee et al. This is an open access article distributed under the Creative Commons Attribution License, which permits unrestricted use, distribution, and reproduction in any medium, provided the original work is properly cited.

Dye-sensitized solar cells (DSSC) are emerging low-cost, simple alternatives to conventional solar cells. While there has been considerable study on improving the efficiency of DSSCs, there has not been sufficient research on a photovoltaic power conditioning system adaptable to DSSCs or on a solar simulator for DSSCs. When DSSCs are commercialized in the near future, the DSSC modules must be connected to an adaptable power conditioning system in order to manage the energy produced and provide a suitable interface to the load. In the process of developing a power conditioning system, a solar simulator with the characteristics of DSSCs is essential to show the performance of the maximum power point tracking. In this paper, a virtual DSSC is designed and simulated in PSIM. Irradiation factors, temperature and shadow effects are considered in dynamic link library block in PSIM which is linked to the external C routine. A 100 W converter is built to show the performance of a DSSC as the solar simulator controlled by a digital signal processor.

## 1. Introduction

Solar energy has emerged as a solution for problems such as depletion of fossil energy resources and environmental pollution. Solar energy is a clean and permanent energy source. In addition, solar power systems have many benefits such as very low maintenance, long life, and easy installation. That is why the solar power industry is rapidly developing [1]. Most solar panels on the photovoltaic market are crystalline or multicrystalline silicon solar cells. However, in spite of their high efficiency, these are difficult to commercialize due to shortage of raw materials, high manufacturing costs, and complicated fabrication processes. DSSCs based on a photochemical mechanism are in the limelight as a promising alternative to silicon solar cells because of various advantages such as low manufacturing costs, simple fabrication process, flexibility, and transparency [2–4]. However, to commercialize DSSCs, there are still many shortages to overcome [5]. In particular, their low efficiency limits their practical application. Much DSSC research is

currently focused on this problem. In addition, research on the installation of large-scale DSSC modules is important [6].

To develop a solar controller for DSSCs, researchers need to consider the output characteristics and conduct an experiment with DSSC modules. However, the output characteristics of DSSCs depend on the weather conditions. Therefore, an assistant power system that simulates the characteristics of DSSCs and that can be controlled arbitrarily by the researcher is required in the development process for reliable experimental data.

To solve these problems, in this paper, a simple and low-cost DSSC solar simulation of discontinuous conduction mode (DCM) boost converter is suggested, showing the performance versus such factors as irradiance, temperature, shading, and connection method. The algorithm is first simulated by the DLL block linked with the external C routine, referring to the extracted data from lab-made DSSCs. The simulation program shows the  $I$ - $V$  and  $P$ - $V$  curves versus conditions. The proposed solar simulator consists of

the power supply, DC-DC boost converter, electronic load, and digital signal processor (DSP). That system generates the output power to 100 W level of DSSCs controlled by DSP with the SS algorithm. The SS is designed for trial experiments of large scale, and the reliability of the SS is verified in this paper.

## 2. Dye-Sensitized Solar Cell

**2.1. An Equivalent Circuit of DSSCs.** The simple equivalent circuit consists of the current source, diode, capacitances, and the resistances. The current source generates the  $I_{PH}$  (photoelectric current) in proportion to the irradiation of sunlight. Figure 1 shows the equivalent circuit of a DSSC. The  $C_{Pt}$  and  $R_{Pt}$  are the impedance through carrier transport on the surface of the counter electrode. The  $C_{ELEC}$  and  $R_{ELEC}$  are the impedance with regard to carrier transport through the ions in the electrolyte, and those are worked as the diode with regard to electron transfer of  $TiO_2$ /dye/electrolyte facing surface.  $R_{TCO}$  is the resistance through the surface resistance.  $R_{SH}$  is shunt resistance through the back electron transfer. The capacitance elements can be ignored because the values of the capacitances are fairly large. That is why the circuit will be simplified such as current source, diode, one of parallel resistance, and three of series resistances. The Equation (1) represents the  $I_D$  which is the current flowing through a diode:

$$I_D = I_O \left\{ \exp \left( q \frac{V + IR_S}{nkT} \right) - 1 \right\}. \quad (1)$$

Equation (2) represents the  $I_{SH}$  which is current flowing through  $R_{SH}$ . The  $R_{TCO}$ ,  $R_{ELEC}$ , and  $R_{Pt}$  are incorporated as  $R_S$ :

$$I_{SH} = \frac{V + IR_S}{R_{SH}}. \quad (2)$$

The output current  $I_O$  can be explained like (3). The output current is same as all current excluding  $I_D$  and  $I_{SH}$  [7–9]:

$$I_O = I_{PH} - I_D - I_{SH} = I_{PH} - I_D \left\{ \exp \left( q \frac{V + IR_S}{nkT} \right) - 1 \right\} - \frac{V + IR_S}{R_{SH}}. \quad (3)$$

**2.2. The Characteristics of DSSCs.** The characteristics of DSSCs are changed according to the factors such as irradiation, temperature, shadowing effect, and connecting style. In this paper, the characteristics of a  $1 \times 1 \text{ cm}^2$  size DSSC unit cell are explained according to some factors. Figure 2 shows  $1 \times 1 \text{ cm}^2$  size lab-made DSSC unit cell.

**2.2.1. The Shadowing Effect.** The shadowing effects affect the characteristics of a DSSC. When the DSSC is under the shadow, power loss is generated as heat because of reverse current flows [10–12]. But a DSSC is less sensitive to partial shade compared with the Si solar cells.

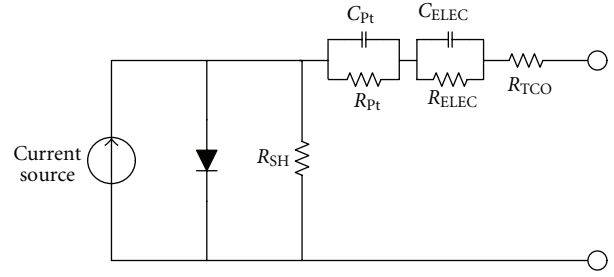


FIGURE 1: An equivalent circuit of a DSSC.

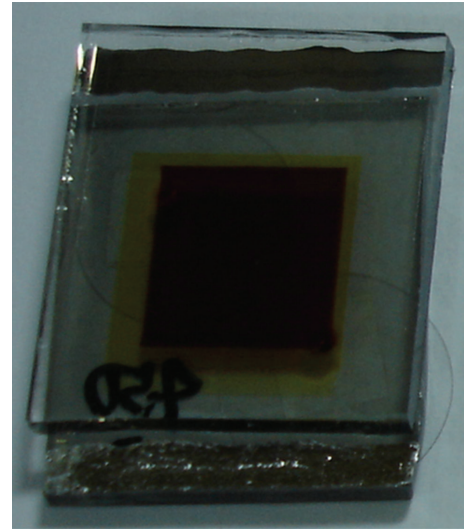


FIGURE 2: A  $1 \times 1 \text{ cm}^2$  size DSSC unit cell.

A  $1 \times 1 \text{ cm}^2$  DSSC was prepared for experiments on the shadowing effect. The metal-coated foil was also prepared to create a shadow. The shadowing effects were given to 0, 25, 50, and 75% in order. The photovoltaic performances of the cell were evaluated by a source meter unit (Model 2400, Keithley Instruments Inc.) under the standard test conditions (STC), which is the temperature of  $25^\circ\text{C}$  and irradiation of  $1000 \text{ W/m}^2$ , using a solar simulator (Sun 2000, Abet Technologies Inc., USA). Table 1 shows the characteristics of the unit cell according to the shadowing effects such as open-circuit voltage ( $V_{oc}$ ), short-circuit current ( $I_{sc}$ ), fill factor (FF), efficiency, and maximum power. The current is greatly reduced by increasing the shadowing rate. But the voltage is a little reduced. The power is reduced according to the shading rate. The  $V_{oc}$  and  $I_{sc}$  of each shading condition are considered in SS algorithm.

**2.2.2. The Temperature and Irradiation Effect.** The DSSCs in the field operate under the variable STC due to the irradiation and temperature changes throughout the day.

TABLE 1: The characteristics of the unit cell according to the shadowing effect.

Shading rate	Parameter				
	$V_{oc}$ (V)	$I_{sc}$ (mA)	FF	$\eta$ (%)	$P_{max}$ (mW)
0%	0.734	8.186	0.643	3.863	3.863
25%	0.722	5.932	0.664	2.843	2.843
50%	0.716	4.026	0.707	2.039	2.093
75%	0.702	2.631	0.738	1.363	1.363

The change of temperature and irradiation affects the efficiency and performance of a DSSC. Figure 3(a) shows the  $I$ - $V$  characteristics of a DSSC according to the change of the temperature. At this time, the irradiation is constant at  $1000 \text{ W/m}^2$ . The current is almost constant, and the voltage is changed by the change of the temperature. The voltage decreases by approximately  $2.84 \text{ mV}$  when the temperature increases by  $1^\circ\text{C}$  [13]. The maximum power point is also changed by the alternation of the value of voltage. Figure 3(b) shows the  $I$ - $V$  characteristics of a DSSC according to the change of the irradiation. At this time, the temperature is constant as  $25^\circ\text{C}$ . The voltage is almost constant, but the current is linearly changed according to the irradiation. The maximum power point is also changed by the value of irradiation.

**2.2.3. The Series-Parallel Connection.** We assumed that there is no loss in series-parallel connection. The value of the voltage increases in proportion to the number of DSSCs in the series connection. At this time, the current is constant. And the value of the current increased in the parallel connection. At this time, the voltage is constant. Therefore, the  $I$ - $V$  and  $P$ - $V$  characteristics of DSSCs according to the connection method can be simply obtained by multiplying  $N_s$  (Number of series connections) and  $N_p$  (Number of parallel connections) to STC data.

### 3. Simulation Program

**3.1. The Design of the Simulation Program.** The SP (simulation program) model is designed with DLL block in the PSIM and Microsoft Visual C++. The DLL block is the virtual circuit of the  $1 \times 1 \text{ cm}^2$  DSSC unit cell. The DLL block is the linked external C routine which is made from Microsoft Visual C++. The results of the simulation are represented as  $I$ - $V$  and  $P$ - $V$  curves according to the input conditions such as irradiation, temperature, connection style, and shadow effect. Figure 4 shows PSIM circuit with a DLL block and the window for conditions input.

Since characteristic equations of DSSC are of nonlinear form, the implementation using equivalent equations take lots of data memory size and calculation time in microcontroller unit (MCU). So, the proposed method uses only extracted data from lab-made DSSC according to the factors and interpolation method to obtain the new reference curve in any conditions [14].

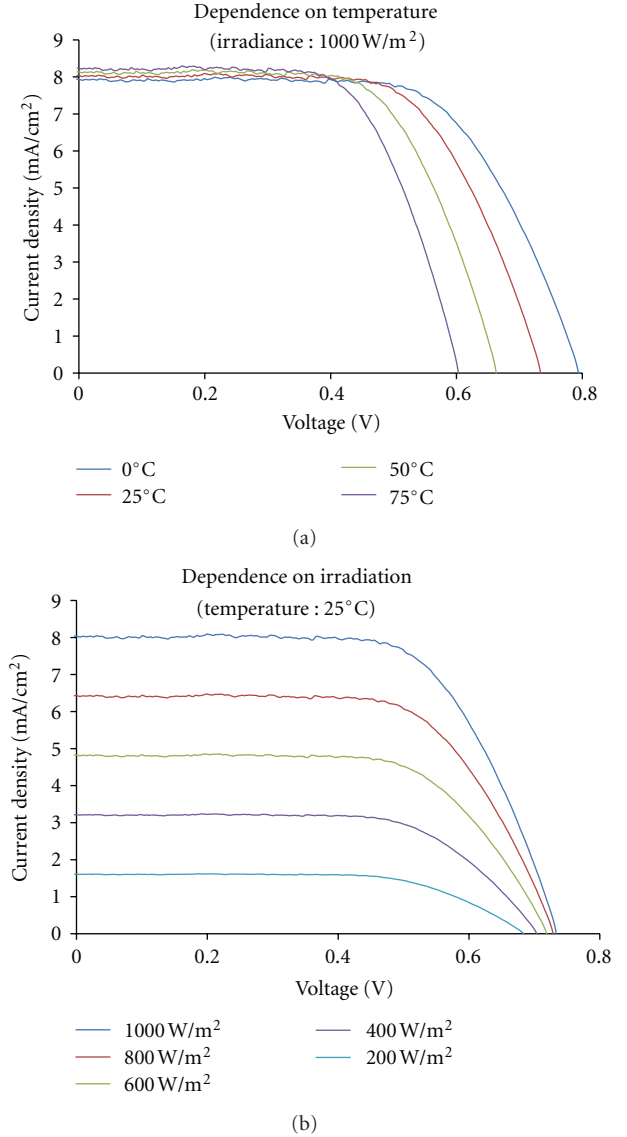


FIGURE 3: (a) The  $I$ - $V$  characteristic curves of DSSCs according to the temperature. (b) The  $I$ - $V$  characteristic curves of DSSCs according to the irradiation.

To simplify the process of getting  $I$ - $V$  curve in selected new conditions, relationship variables are calculated from Figure 5:

$$V_{IrrN} = V_{IrrL} - \frac{Irr - Irr_L}{Irr_H - Irr_L} (V_{IrrL} - V_{IrrH}), \quad (4)$$

$$V_{TN} = V_{TL} - \frac{T - T_L}{T_H - T_L} (V_{TL} - V_{TH}), \quad (5)$$

$$V_{SHN} = V_{SHL} - \frac{SH - SH_L}{SH_H - SH_L} (V_{SHL} - V_{SHH}), \quad (6)$$

$$\beta_{Irr} = \frac{V_{IrrN}}{V_{STC}}, \quad \beta_T = \frac{V_{TN}}{V_{STC}}, \quad \beta_{SH} = \frac{V_{SHN}}{V_{STC}}, \quad (7)$$

where  $V_{IrrL}$  is the voltage of the lower range according to the selected irradiation,  $V_{IrrH}$  is the voltage of the higher

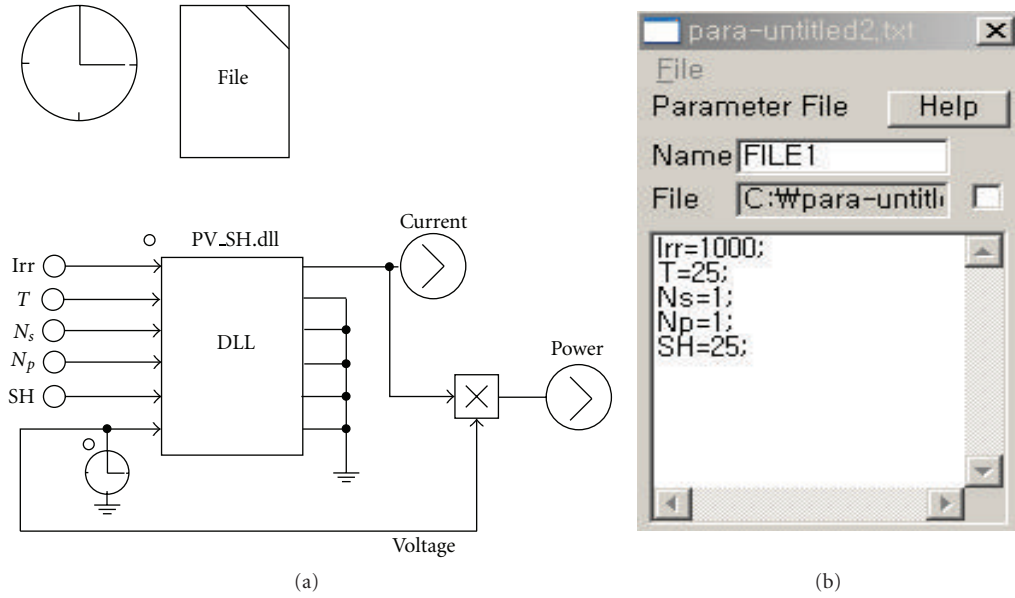


FIGURE 4: (a) The SP model with DLL block. (b) The window for conditions input.

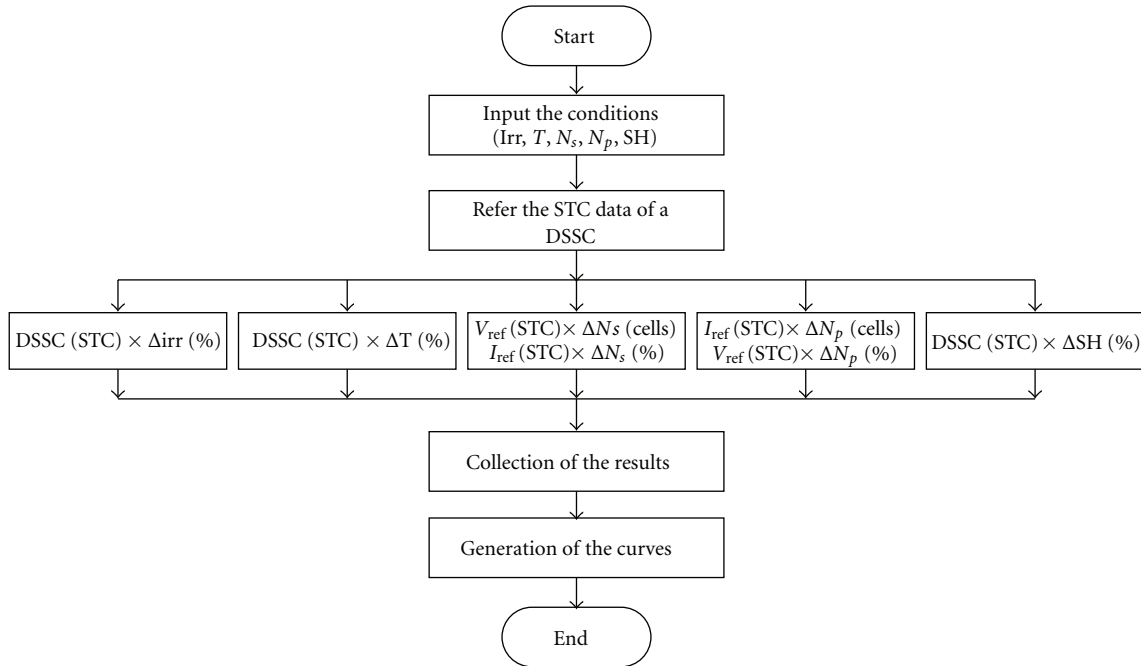


FIGURE 5: Proposed SS algorithm flow chart.

range according to the selected irradiation,  $V_{IrrN}$  is the new reference voltage according to the selected irradiation, Irr is the selected value of irradiation,  $V_{TL}$  is the voltage of the lower range according to the selected temperature,  $V_{TH}$  is the voltage of the higher range according to the selected

temperature,  $V_{TN}$  is the new reference voltage according to the selected temperature, T is the selected value of temperature,  $V_{SHL}$  is the voltage of the lower range according to the selected shadowing rate,  $V_{SHH}$  is the voltage of the higher range according to the selected shadowing rate,

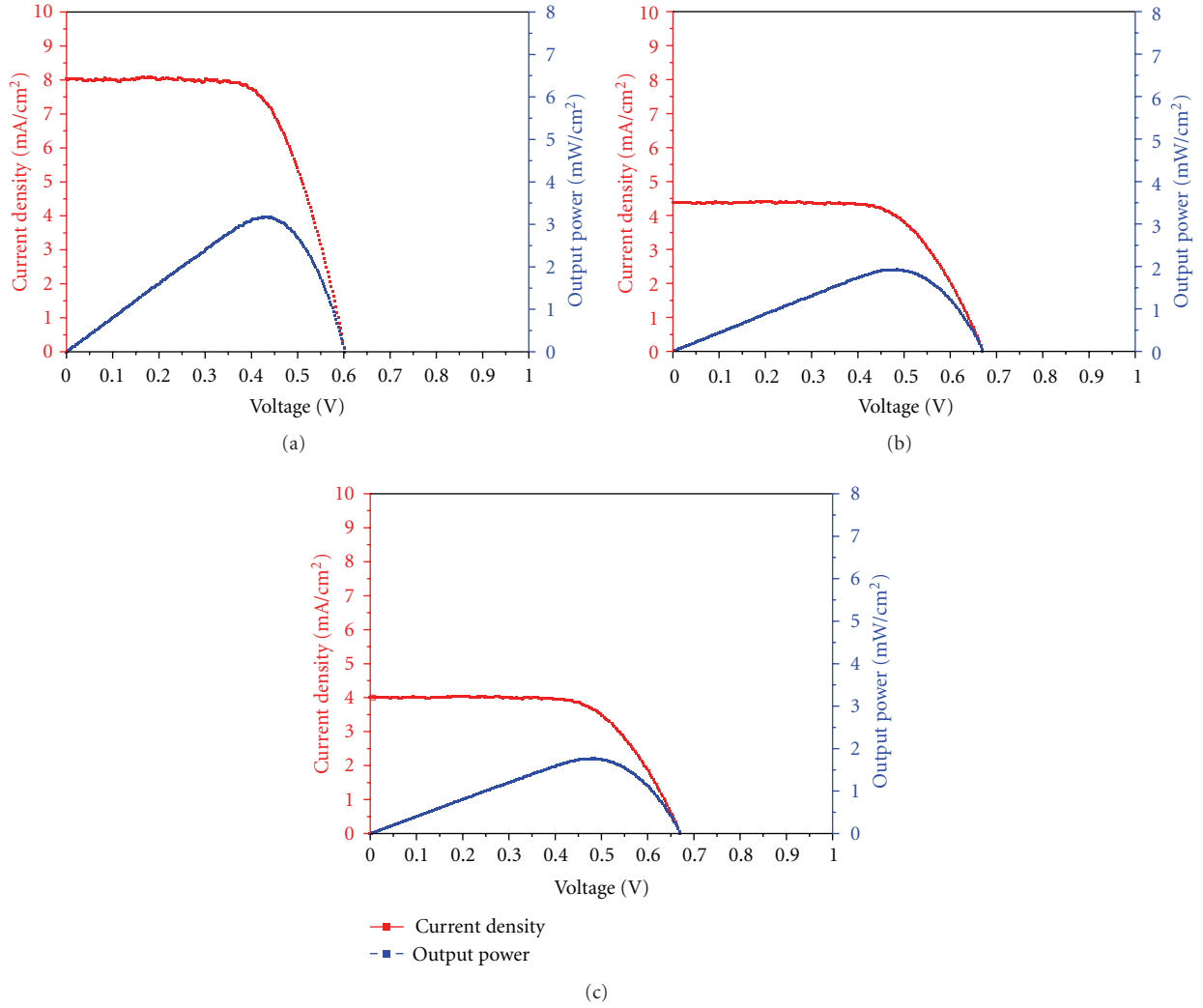


FIGURE 6: (a) Simulation results at 75°C, 1000 W/m<sup>2</sup>, 0% shadowing rate. (b) Simulation results at 25°C, 600 W/m<sup>2</sup>, 0% shadowing rate. (c) Simulation results at 25°C, 1000 W/m<sup>2</sup>, 50% shadowing rate.

$V_{SHN}$  is the new reference voltage according to the selected shadowing rate, SH is the selected value of shadowing rate,  $\beta_{irr}$  is the relationship variable of irradiation,  $\beta_T$  is the relationship variable of temperature,  $\beta_{SH}$  is the relationship variable of shadowing rate, and  $V_{STC}$  is the voltage at STC. For example, if the irradiation is selected to 700 W/m<sup>2</sup>, the higher range and lower range are each 800 W/m<sup>2</sup> and 600 W/m<sup>2</sup>.

Finally, the new reference voltage ( $V_{REF}$ ) is calculated by

$$V_{REF} = V_{STC} \times (\beta_{irr} \times \beta_T \times \beta_{SH}) \times N_s. \quad (8)$$

Similarly, the new reference current ( $I_{REF}$ ) is obtained through the same procedure like (4) ~ (8):

$$I_{REF} = I_{STC} \times (\alpha_{irr} \times \alpha_T \times \alpha_{SH}) \times N_p, \quad (9)$$

where  $\alpha_{irr}$  is the relationship variable of irradiation,  $\alpha_T$  is the relationship variable of temperature,  $\alpha_{SH}$  is the relationship variable of shadowing rate, and  $I_{STC}$  is the current at STC.

After the calculation is finished according to the conditions, the collection of the results will be made. After the collection is finished, the results of simulation will be displayed at the Simview of the PSIM.

**3.2. The Result of the Simulation Program.** The output of DSSCs is changed according to some factors. The SP model represents the output of DSSCs in the PSIM. The results of simulation are displayed at the Simview of the PSIM according to some factors. Figure 6 shows the  $I$ - $V$  and  $P$ - $V$  curves of the simulation for DSSCs. The user can obtain any output curves according to any value of the factors from SP.

## 4. Solar Simulator

**4.1. The Design of the Solar Simulator.** Figure 7 shows the block diagram of the SS. The SS consists of the power supply

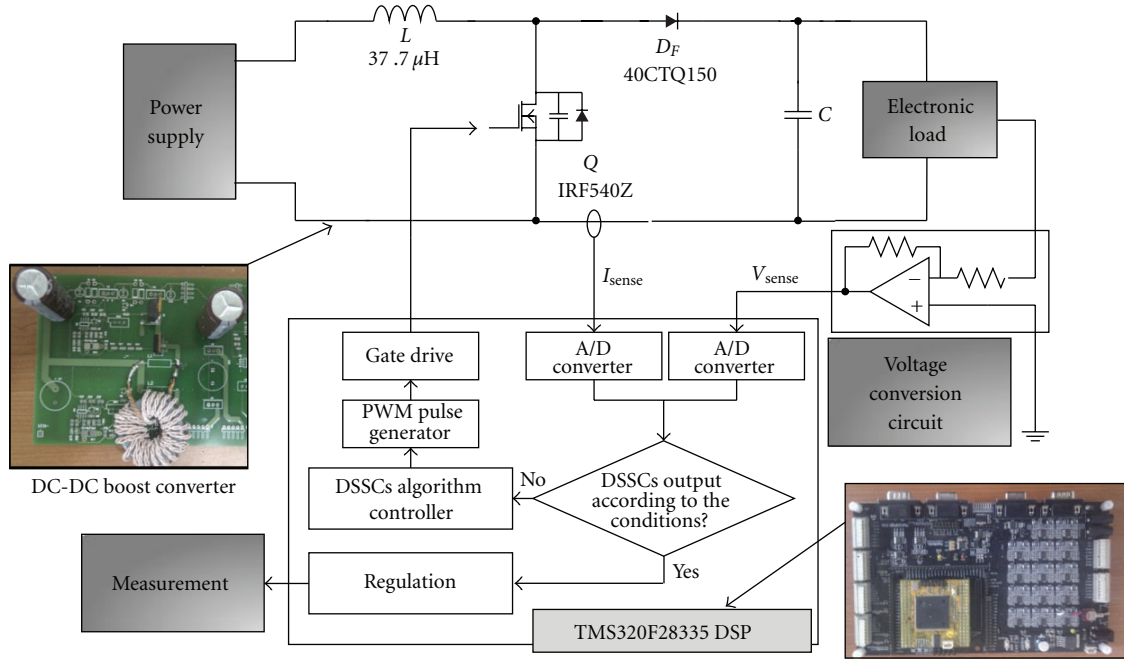
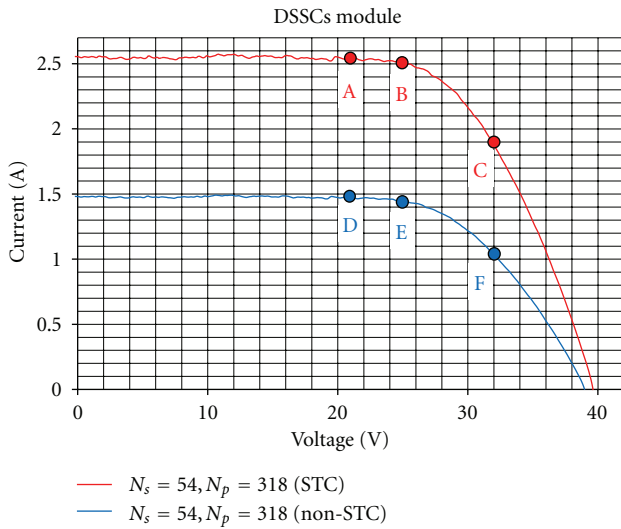


FIGURE 7: The block diagram of the SS.

FIGURE 8: The  $I$ - $V$  characteristic curves of DSSCs module ( $N_s = 54$ ,  $N_p = 318$ ).

device, DC-DC boost converter, electronic load, voltage conversion circuit, and DSP.

The power supply device supplies the power to the entire system. The DC-DC boost converter in DCM is used to

obtain the power of the DSSCs. The basic converter usually uses the hard switching which causes the switching loss and diode recovery loss when the switch is turned on and off [15]. The DCM is not perfect soft switching. However, it is simple to control, only need output voltage to feedback, and is sometimes the best topology given the capacity and switching loss. That is why the DC-DC boost converter in DCM is applied in this paper [16].

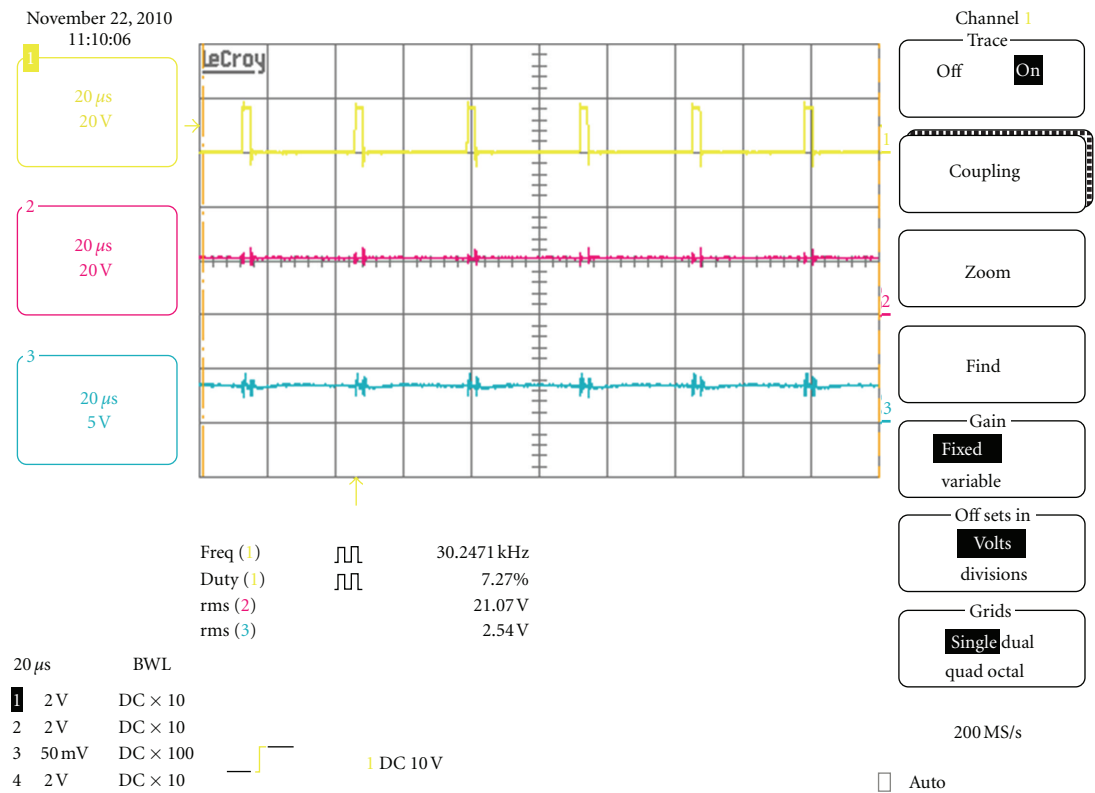
The inductor of DCM boost converter was designed:

$$L = \frac{0.64R_O V_i^2 (V_O - V_i)}{2f V_O^3}, \quad (10)$$

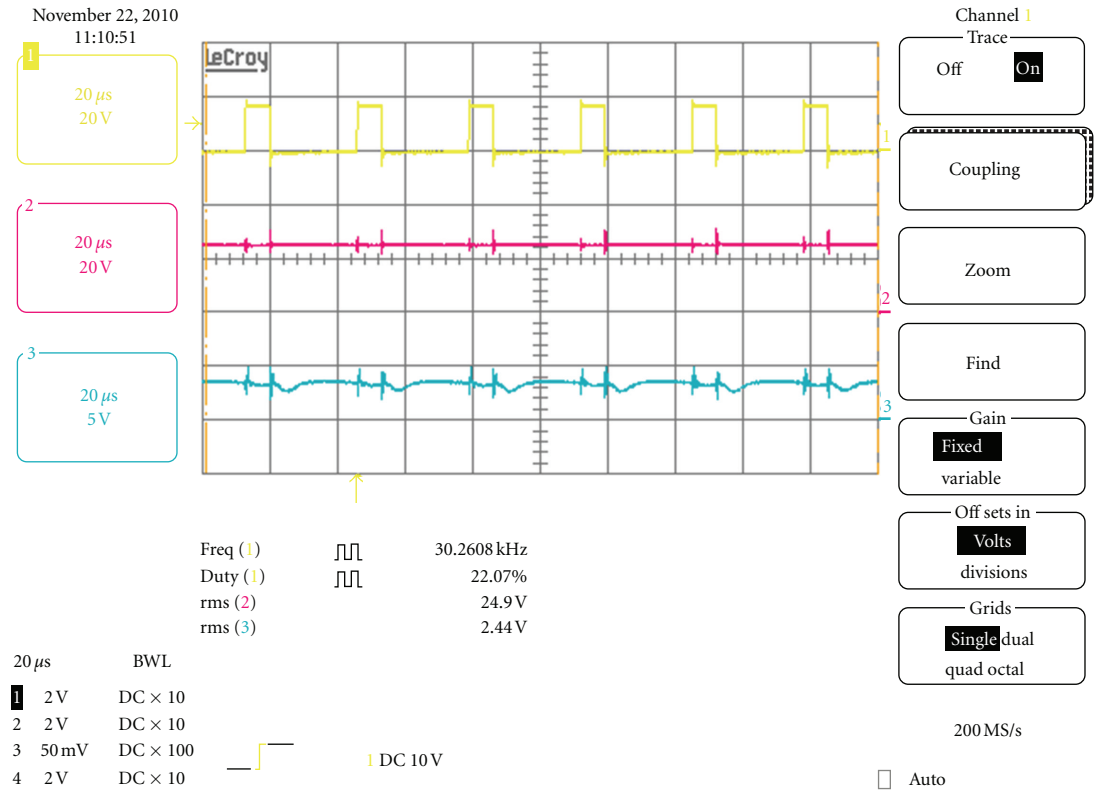
where  $L$  is the value of inductor in DCM,  $R_O$  is the output load,  $V_i$  is the input voltage,  $V_O$  is the output voltage with maximum value of 40 V, and  $f$  is the switching frequency of the converter with the value of 30 kHz.

A converter was implemented on lab-made PCB. The electronics load is used to change the output load condition. In this paper, that DSP (TMS320F28335 EVM) is used to control the current and voltage of the converter. The voltage is measured to the ADC of the DSP through the voltage interface board. A DSP compares the voltage with the reference curve of DSSCs according to the conditions such as the irradiance, temperature, connection method, and shadowing effects and generates the PWM signal to control the reference current in boost converter through the simple PI control. Finally, the converter makes the output of DSSCs and then the measurement is implemented. The output of





(a)



(b)

FIGURE 9: Continued.

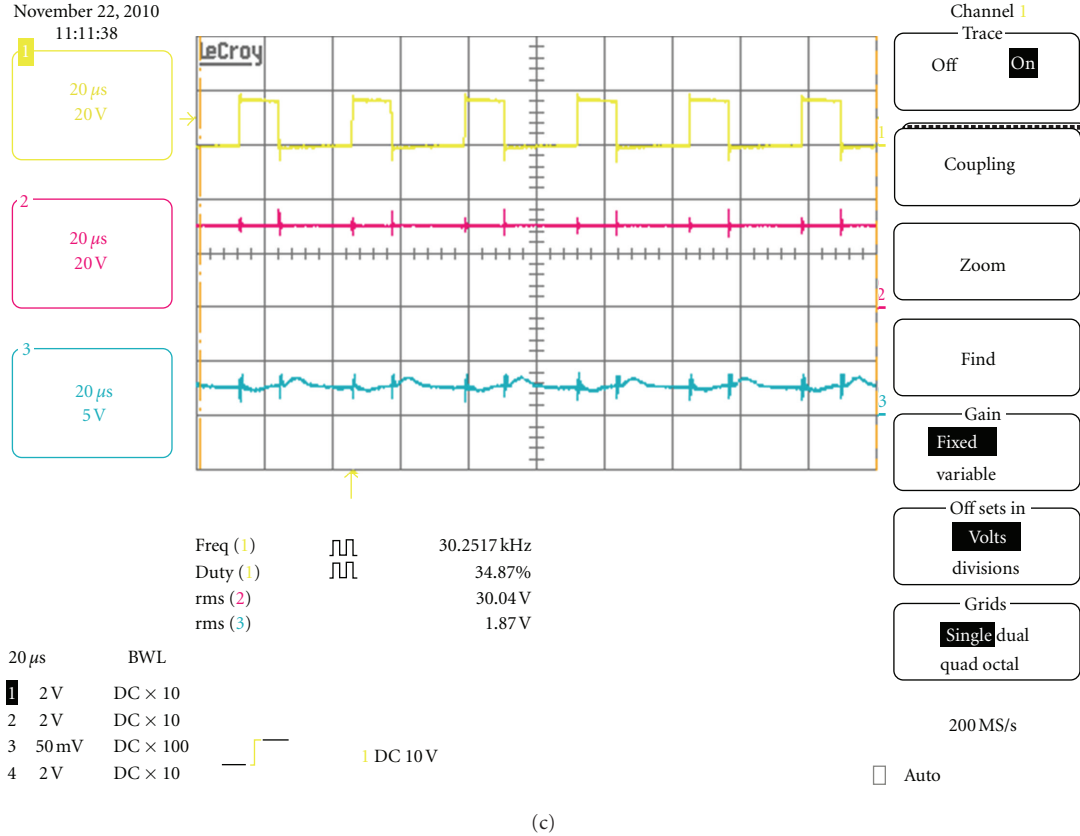


FIGURE 9: (a) The wave forms of 21 V and 2.54 A at Point A. (b) The wave forms of 25 V and 2.44 A at Point B. (c) The wave forms of 30 V and 1.87 A at Point C.

DSSCs can be changed according to change of the value of the electronics load as explained previously.

**4.2. Experimental Results.** Figure 8 shows the  $I$ - $V$  curve (red line) of DSSCs module under STC and the  $I$ - $V$  curve (blue line) of DSSCs module under non-STC. The module consists of 54 series-318 parallel connection without shadowing effects. Six points from A to F are marked on Figure 8, which is the experiment target.

As shown in Figure 9, there are three different wave forms. The first wave form shows the wave form of the gate ( $V_{gs}$ ). The second and third wave forms show the wave forms of the output voltage and current. Figure 9(a) shows the wave forms of 21 V and 2.54 A, which is in Point A. Figure 9(b) shows the wave forms of 25 V and 2.44 A, which is in Point B. Figure 9(c) shows the wave forms of 30 V and 1.87 A, which is in Point C. The outputs of DSSCs are confirmed according to the DSP control with the proposed algorithm.

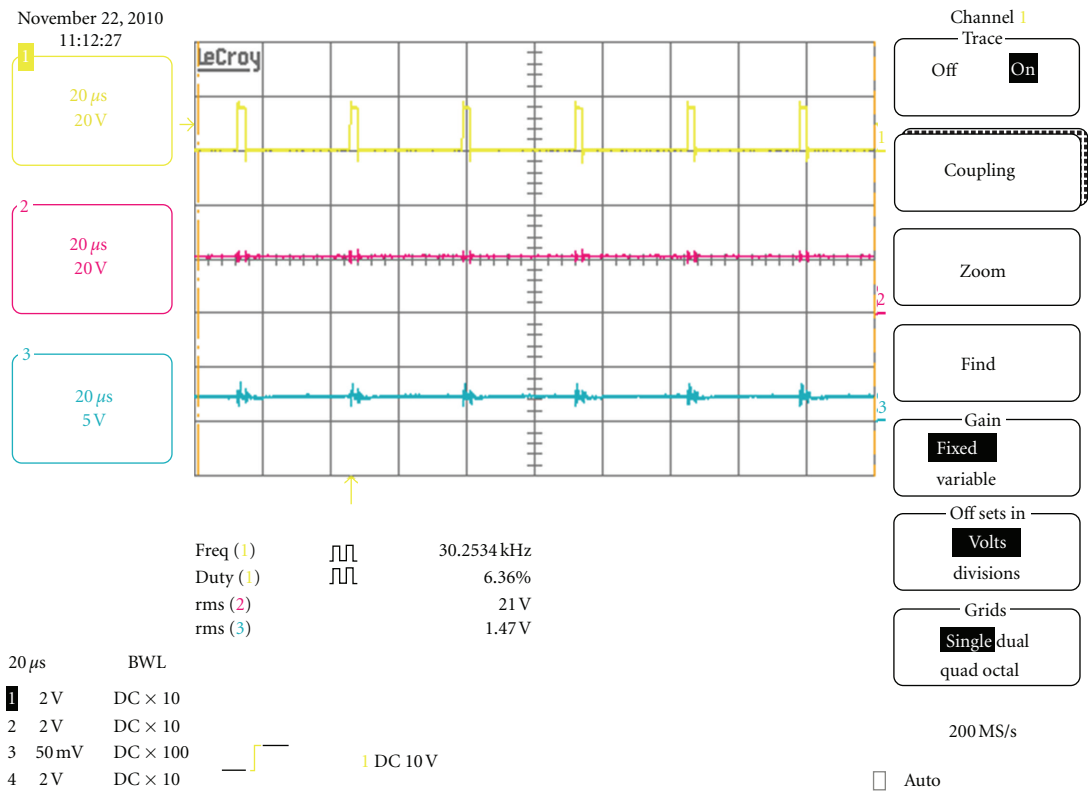
Figure 10 shows the wave forms of the results according to selected irradiation, temperature, and shadowing effect. This module is also DSSCs of the 54 series-318 parallel connected module. At this time, the irradiation is  $800 \text{ W/m}^2$ , the temperature is  $25^\circ\text{C}$ , and the shadowing rate is 25%.

Figure 10(a) shows the wave forms of 21 V and 1.47 A, which is in Point D. Figure 10(b) shows the wave forms of 25 V and 1.43 A, which is in Point E. Figure 10(c) shows the wave forms of 30 V and 1.17 A, which is in Point F. The outputs of DSSCs under non-STC are also confirmed with the proposed SS system.

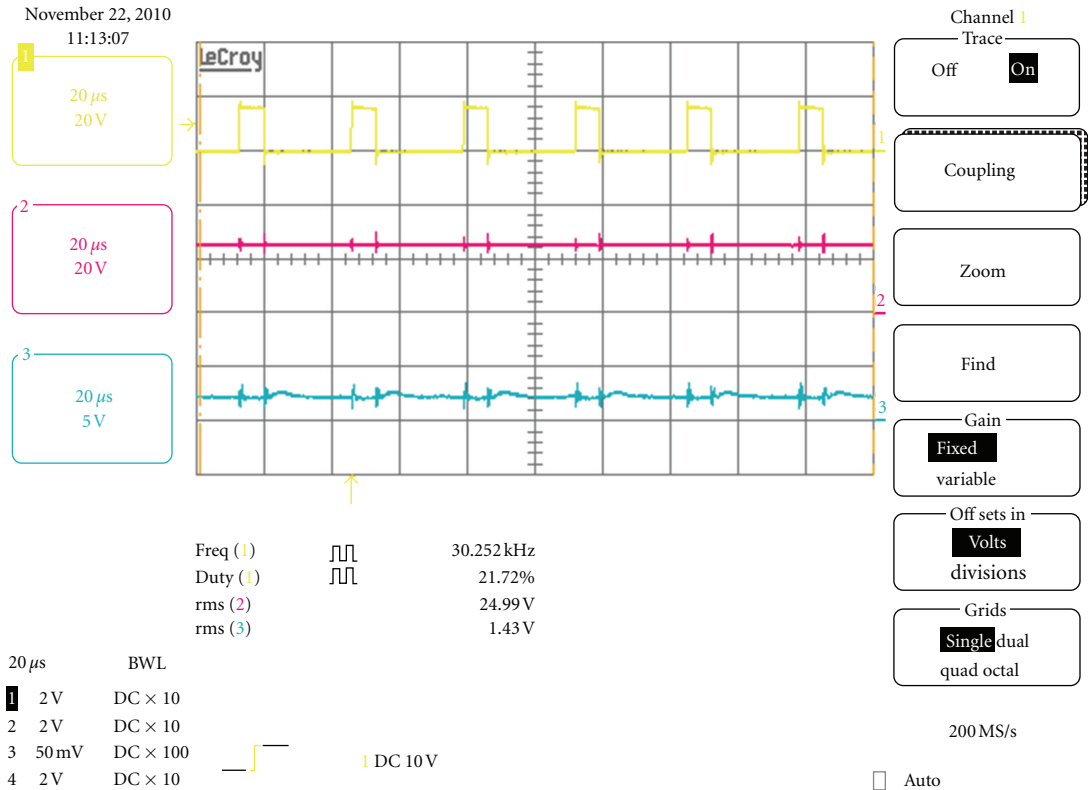
## 5. Conclusion

In this paper, the simple and low-cost SS is suggested for trial test of the DSSCs for developing adaptable power conditioning system. For the first time, the simulation program is designed to simulate the DSSCs. That consists of the DLL block which is linked with the external C routine in the PSIM. The proposed method is based on the actual data from lab-made DSSC unit cell and simple calculation using interpolation method. The SS consists of the power supply, DC-DC boost converter in DCM, electronics load, and DSP. The performance of SS for DSSC modules was verified through the 100 W level of DCM boost converter according to the factors of irradiation, temperature, and shadow effects.



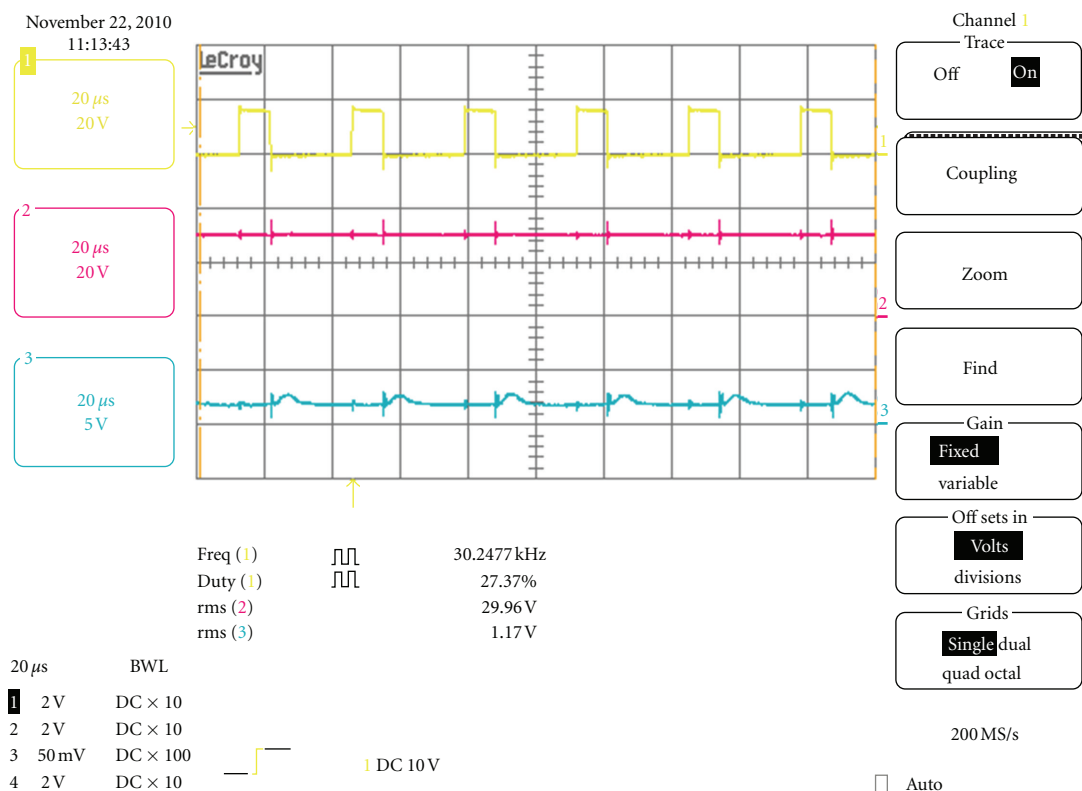


(a)



(b)

FIGURE 10: Continued.



(c)

FIGURE 10: (a) The wave forms of 21 V and 1.47 A at Point D. (b) The wave forms of 25 V and 1.43 A at Point E. (c) The wave forms of 30 V and 1.17 A at Point F.

## Acknowledgment

This work no. 20110001295 was supported by Mid-career Researcher Program through NRF grant funded by the MEST.

## References

- [1] M. Jung Park, "Optimization for Multi array photovoltaic system," *Theories and Applications of Chemical Engineering*, vol. 12, no. 2, pp. 1528–1531, 2006.
- [2] B. O'Regan and M. Grätzel, "A low-cost, high-efficiency solar cell based on dye-sensitized colloidal  $\text{TiO}_2$  films," *Nature*, vol. 353, no. 6346, pp. 737–740, 1991.
- [3] M. Grätzel, "Conversion of sunlight to electric power by nanocrystalline dye-sensitized solar cells," *Journal of Photochemistry and Photobiology A*, vol. 164, no. 1–3, pp. 3–14, 2004.
- [4] M. Grätzel, "Solar energy conversion by dye-sensitized photovoltaic cells," *Inorganic Chemistry*, vol. 44, no. 20, pp. 6841–6851, 2005.
- [5] H. Wang, Y. Liu, H. Xu et al., "An investigation on the novel structure of dye-sensitized solar cell with integrated photoanode," *Renewable Energy*, vol. 34, no. 6, pp. 1635–1638, 2009.
- [6] S. K. Dhungel and J. G. Park, "Optimization of paste formulation for  $\text{TiO}_2$  nanoparticles with wide range of size distribution for its application in dye sensitized solar cells," *Renewable Energy*, vol. 35, no. 12, pp. 2776–2780, 2010.
- [7] L. Han, N. Koide, Y. Chiba, A. Islam, and T. Mitate, "Modeling of an equivalent circuit for dye-sensitized solar cells: improvement of efficiency of dye-sensitized solar cells by reducing internal resistance," *Comptes Rendus Chimie*, vol. 9, no. 5–6, pp. 645–651, 2006.
- [8] H. Seo, M. K. Son, K. J. Lee, J. Kim, J. T. Hong, and H. J. Kim, "A study on the improvement of the efficiency of dye-sensitized solar cell using the laser scribing and the grid electrode," *Transactions of the Korean Institute of Electrical Engineers*, vol. 57, no. 10, pp. 1802–1806, 2008.
- [9] T. O. Saetre, O. -M. Midtgård, and G. H. Yordanov, "A new analytical solar cell I-V curve model," *Renewable Energy*, vol. 36, no. 8, pp. 2171–2176, 2011.
- [10] A. Catani, *Shading Losses of Building Integrated Photovoltaic Systems*, Centre of Applied Research Sustainable Energy Technologies, 2007.
- [11] S. Silvestre, A. Boronat, and A. Chouder, "Study of bypass diodes configuration on PV modules," *Applied Energy*, vol. 86, no. 9, pp. 1632–1640, 2009.
- [12] A. K. Sharma, R. Dwivedi, S. K. Srivastava, and C. M. Pathak, "Performance analysis of a modified solar array under shadow conditions," *Renewable Energy*, vol. 4, no. 2, pp. 257–260, 1994.
- [13] A. Usami, S. Seki, Y. Mita, H. Kobayashi, H. Miyashiro, and N. Terada, "Temperature dependence of open-circuit voltage in dye-sensitized solar cells," *Solar Energy Materials and Solar Cells*, vol. 93, no. 6–7, pp. 840–842, 2009.
- [14] J.-J. Kim, B.-D. Min, J.-P. Lee, T.-J. Kim, D.-W. Yoo, and E.-H. Song, "A novel method of simulation of PV characteristic

curves for PV simulator,” in *Proceedings of the Korean Institute of Power Electronics Conference (KIPE '07)*, pp. 181–183, 2007.

- [15] E.-S. Kim, “High frequency soft switching forward DC/DC converter,” in *Proceedings of the Power Electronics Conference*, pp. 19–25, 1999.
- [16] D.-K. Kwak and C. S. Kim, “A study on high efficiency boost DC-DC converter of discontinuous current mode control,” *The Korean Institute of Electrical Engineers*, vol. 54, no. 9, pp. 431–436, 2005.

